Equilibrium of argon plasma particles at high pressure

Faisal Zakky[1],*, Reeky Fardinata[1], Muhammad Safwan Abd Aziz[2]

[1]Department of Physics, Universitas Riau, Pekanbaru 28293, Indonesia
[2]Department of Physics, Universiti Teknologi Malaysia, Johor 81310, Malaysia

ABSTRACT	ARTICLE INFO
The density value and plasma reaction rate are the physical quantities needed to produce plasma. Both are used to estimate the heat energy and operating time of the plasma. Argon plasma at atmospheric pressure is widely used in industry. Density values and plasma reaction rates were obtained by computational modeling using the continuity equation and the Arrhenius equation obtained from experimental data. Five argon species were used in this research including Ar^*, Ar^+, Ar_2^+, Ar, and electron. Plasma equilibrium occurs in time intervals of $10^{-12} - 10^{-3}$ seconds with a temperature of 2 eV. The overall thermal argon plasma equilibrium density ranges within the interval $10^9 - 10^{16}$ m^{-3}. The value of the fastest reaction rate obtained is equal to 2.482×10^4 m^{-3}.s^{-1} until the smallest reaction rate is obtained equal to 14.613×10^{-34} m^{-3}.s^{-1}.	 *This is an open access article under the [CC BY](#) license.*

* Corresponding Author

E-mail address: faisal.zakky2867@student.unri.ac.id

1. INTRODUCTION

As early as 1920, Irving Langmuir described plasma as a form of natural electricity consisting of ions and electrons and having the ability to produce electric and magnetic fields. Almost 99% of what exists in the universe is plasma, therefore many scientists are trying to perfect it so that it can benefit human life [1]. Plasma has several broad and very attractive advantages, including having excellent precision, supplying relatively low energy, enabling large-scale processes, and having a very simple and effective control system [2-3].

Plasma equilibrium can be achieved if the process is accompanied by the influence of radiation or particle collisions are always accompanied by a reverse process. Plasma in equilibrium conditions will follow the distribution and radiation laws [4-5]. Plasma can be classified into two, namely low-pressure plasma (vacuum) and high-pressure plasma (atmosphere). This research is a high-pressure plasma with a pressure value of 1 atm (atmosphere) [6-7]. In this research, argon gas is used which will be operated at high pressure.

Argon plasma is one of the most commonly used types of plasma for cleaning because of its cheap price, ability to prevent oxidation, and wide availability [8-9]. In the argon species, the density and characteristics that will be looked for are electrons (e), argon ions (Ar^+), argon molecular ions (Ar_2^+), excited argon atoms (Ar^*), and argon atoms (Ar). In this equilibrium, the degree of plasma ionization is determined, which will be modeled computationally to solve the argon gas plasma reaction equation using the Runge-Kutta method, while the solution means using the help of MATLAB. The Runge-Kutta method is used to solve the continuity equation which depends on time to obtain the equilibrium density value for each species. The Runge-Kutta method provides solutions to differential equations with smaller growth in truncation error (percentage error).

2. LITERATURE REVIEW

2.1. Definition of Plasma

Plasma is a condition where a gas experiences what is called ionization, which indicates the conversion of neutral atoms or molecules into electrons and ions so that they become free radicals or active species [10]. Each atom of ordinary gas contains the same amount of positive and negative charge. Gas becomes plasma when the addition of heat or energy causes a large number of atoms to release some or all of their electrons[11]. Plasma is also known as fourth phase matter after the solid, liquid, and gas, which are illustrated in Figure 1. In this case, it completes the pressure correction to the ideal gas equation which applies to plasma conditions where plasma is a new state [12].
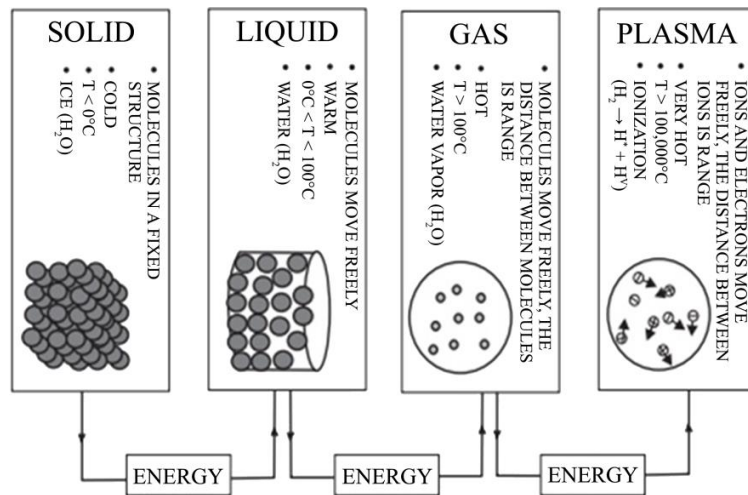

Figure 1. Plasma as the fourth phase.

2.2. Plasma Classification

There are several types of plasma, natural or artificial, that extend from stars, winds, the solar corona, and the Earth's ionosphere to high-pressure arc regions. The types of plasma differ, especially in electron density and average electron energy, which can be seen in Figure 2 below [11]. Figure 2 illustrates the characteristics of several artificial and natural plasmas in terms of electron temperature and density [13].
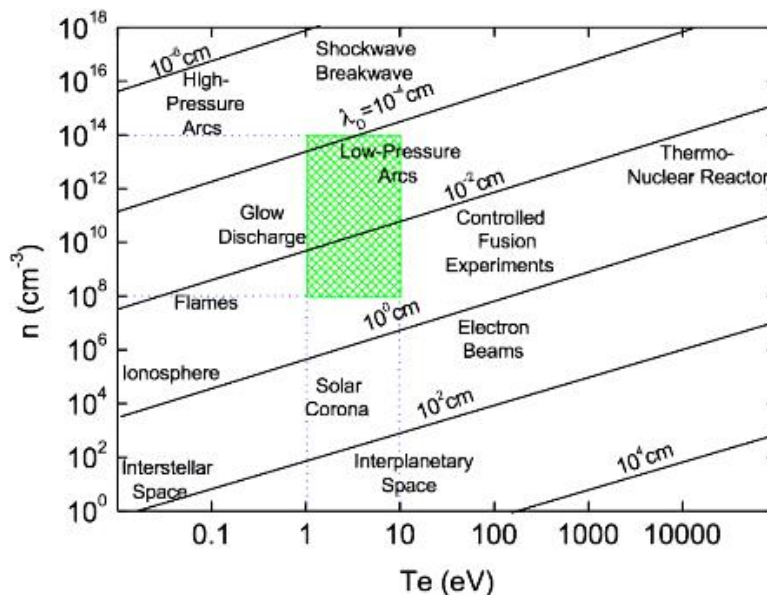

Figure 2. Typical plasma is characterized by energy and electron density.

2.3. Plasma Characteristics

Plasma consists of many types of particles (species). Apart from neutral ground state atoms and molecules, there can be various excited species, positive or negative ion species, and of course, electrons that sustain the plasma [14]. Complexity in plasma is expressed as a function of time and a function of space. This complexity is determined by the characteristics of plasma as a collection of charged particles. The kinetic temperature of a species can be formulated as:

$$T_s = \frac{1}{3}m_s < V_s^2 >$$ (1)

Kinetic temperature is generally measured in units of electronvolts (eV) [15]. Plasma has different unique properties that depend on particle interactions, one of the properties is the impact effect. This impact effect with quite large physical phenomena is caused by electromagnetic forces which are quite large so that they influence the particles in the plasma and interact continuously with other charges [16]. Plasma occurs due to the formation of a quasi-neutral mixture of electrons, radicals, positive ions, and negative ions. A quasi-neutral condition is an area where there is an ion density (n_i) that is almost the same as the electron density (n_e) so that it can be said $n_i \approx n_e \approx n$, with n representing the density in general which is called plasma density [1].

Plasma consists of many types of particles (species). Apart from neutral ground state atoms and molecules, there can be various excited species, positive or negative ion species, and electrons that sustain the plasma. Knowing the temperature of individual species and their concentrations is critical for plasma applications [17]. One of the fundamental criteria for equilibrium in a system is that the pressure and temperature are constant and uniform throughout the system. This implies that the condensed phase needs to be in equilibrium with the gas phase, and components in the gas phase must maintain a constant in their partial pressures or concentrations [18]. In plasma particles, we will apply a program that calculates the concentration of individual particle species in a high-pressure argon plasma for a certain electron temperature T_e and gas temperature T_g [19].

Practically, this means that the sum density of each particle species is only a function of time, not position.

$$n_\alpha = n_\alpha(t)$$ (2)

Under the zero-dimensional approach, the continuity equation for the species is simplified to an ordinary differential equation,

$$\frac{\partial n_\alpha}{\partial t} = s_\alpha$$ (3)

Equation 3 looks relatively simple but it should be pointed out that the source term s_α is a complex function of temperature (which is constant in our model) and the sum density of other particle species [8]. In plasma, there is a collective property where the overall charge in the plasma becomes zero. In this neutral plasma condition, the ion charge is the same as the electron charge or $(n_i q_i - n_e e) = 0$ where n_e is the ion density and n_e is the electron density. So the density of negatively charged particles (electrons) is the same as the density of positively charged particles (positive ions) [16].

2.4. Argon Plasma Characteristics

Argon as a noble gas is an inert gas. The number of free electrons (primary electrons) in the plasma space is given an average energy of 4 eV. The species of argon plasma consist of e, Ar^+, Ar_2^+, Ar^*, and Ar. The argon model includes the particle species listed in Table 1 [8]. Equation (2) is solved only for five Ar species, Ar^*, Ar^+, Ar_2^+, and e. The number density of ground state argon can be determined from the equation of state for an ideal gas, which works very well for monatomic gases at high pressure [20]. If argon gas is not ionized, the total density of argon will be:

$$n_{ar} = \frac{P}{k_B T_g}$$ (4)

where P is pressure, k_B is Boltzmann's constant, and T_g is the temperature of the heavy particle. However, the above equation does not apply if part of the argon gas is ionized or as mentioned previously [21].

2.5. Argon Chemical Kinetic Model

The continuity equation is applied to argon species in describing chemical kinetic models. The continuity equation can be written as follows:

$$\frac{dn}{dt} = \nabla.(n\,v) = S \tag{5}$$

The diffusion term $\nabla.(nv)$ in Equation (5) can be ignored in dimensionless atmospheric pressure plasma, so Equation (5) changes to zero dimensions and only depends on time, so the continuity equation can be written:

$$\frac{dn}{dt} = S \tag{6}$$

Equation (6) states that the change in density depends only on the production rate of the species per unit volume (S). A reaction can be expressed by the following equation [22].

$$aA + bB \rightarrow cC + dD \tag{7}$$

Meanwhile, the forward reaction rate is given by:

$$R_f = k_f\,(n_A)^a(n_B)^b \tag{8}$$

The rate of back reaction is given by:

$$R_r = k_r\,(n_C)^c(n_D)^d \tag{9}$$

The species involved in the reaction are expressed in symbols A, B, C, D, and n represent the species density. Meanwhile, a, b, c, and d are the number of molecules of each reactant and the reaction products involved. The production rate of a species C per volume for each reaction in the reaction equation is given by:

$$S_c = (R_f\,x\,c) - (R_r\,x\,0) \tag{10}$$

In general, the reaction rate of product species per unit volume for each reaction can be calculated according to the following equation:

$$S = (M_r - N_f) - (R_f - R_r) \tag{11}$$

where M_r and N_r are the numbers of molecules of the reaction product and reactant species respectively.

2.6. Runge-Kutta method

The 4th Order Runge-Kutta method offers the solution of differential equations with much smaller truncation error growth. In general, the Runge-Kutta method is used to solve problems related to numerical calculations. The general form of the 4th-order Runge-Kutta method can be written as:

$$y_{i+1=}y_i + h(a_1k_1 + a_2k_2 + a_3k_3 + a_4k_4 \tag{12}$$

where a_1, a_2, ..., a_n are constants, h is the step size of each iteration and n is the method order, wherein the 4th order Runge-Kutta method, the values of k_1, k_2, k_3, and k_4 are:

$$k_1 = f(t_i, y_i) \tag{13}$$

$$k_2 = f(t_i + p_1 h, y_i + q_{11} k_1 h) \tag{14}$$

$$k_3 = f(t_i + p_2 h, y_i + q_{21} k_1 h + q_{22} k_2 h) \tag{15}$$

$$k_4 = f(t_i + p_3 h, y_i + q_{31} k_1 h + q_{32} k_2 h + q_{33} k_3 h) \tag{16}$$

3. RESEARCH METHODS

This research was carried out computationally to solve the argon gas plasma reaction equation using the Runge-Kutta method, while the solution was used using the help of MATLAB software.

3.1. Argon Plasma Reaction Data Collection

Argon plasma reaction data is taken from various research references. This reaction data contains the required information about the reaction rate in the reaction. Argon plasma reaction data can be seen in Table 1.

Table 1. Argon plasma gas reaction data.

Reaction	Reaction rate constant	Units
$e + Ar \rightarrow e + Ar^*$	$4.9 \times 10^{-15} \cdot \sqrt{T_e} \cdot \exp(-11.65/T_e)$	m^3/s
$e + Ar^* \rightarrow e + Ar$	$4.8 \times 10^{-16} \cdot \sqrt{T_e}$	m^3/s
$e + Ar \rightarrow 2e + Ar^+$	$1.27 \times 10^{-4} \cdot \sqrt{T_e} \cdot \exp(-15.76/T_e)$	m^3/s
$e + Ar^* \rightarrow 2e + Ar^+$	$1.37 \times 10^{-12} \cdot \sqrt{T_e} \cdot \exp(-4.11/T_e)$	m^3/s
$e + Ar_2^+ \rightarrow Ar + Ar^*$	$1.37 \times 10^{-12} \cdot (T_e/0.026)^{-0.67} \cdot (1 - \exp(-418/T_g))/(1 - 0.31\exp(-418/T_g))$	m^3/s
$e + Ar_2^+ \rightarrow e + Ar + Ar^*$	$1.11 \times 10^{-12} \cdot \exp(-2.94 - 3(T_g - 300)/(11{,}604T_g))$	m^3/s
$Ar^* + Ar^* \rightarrow e + Ar^+ + Ar$	6.2×10^{-16}	m^3/s
$Ar^* + Ar \rightarrow Ar + Ar$	3.0×10^{-16}	m^3/s
$e + e + Ar^+ \rightarrow e + Ar$	$8.75 \times 10^{-39} \cdot T_e^{-4.5}$	m^6/s
$Ar^+ + 2Ar \rightarrow Ar + Ar_2^+$	$2.25 \times 10^{-43} \cdot (T_g/300)^{-0.4}$	m^6/s
$Ar + Ar_2^+ \rightarrow Ar^+ + 2Ar$	$0.522 \times 10^{-15} \cdot T_g^{-1} \cdot \exp(-15{,}131/T_e)$	m^6/s

3.2. Research Flow Diagram

The research flow diagram aims to display the systematic work in research. Figure 3 shows the overall process from the research until the conclusion was reached.
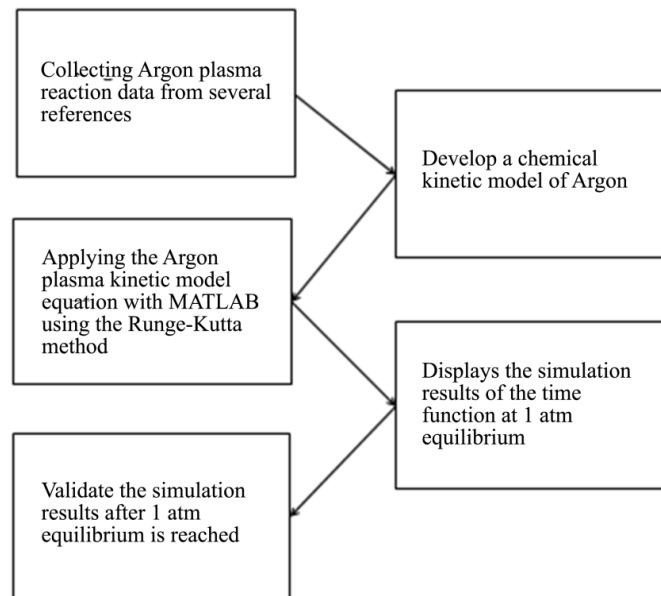

Figure 3. Research flow diagram.

Equilibrium of argon plasma particles at high pressure (**Zakky et al.**)

3.3. Research Procedures

The research consists of several stages. The first stage is to collect argon plasma reaction data and Arrhenius parameters. The chemical kinetic model of argon which has been prepared in Table 1 will be placed into the MATLAB program coding.

3.4. Research Program Coding

Computational coding consists of the main data program and input. The main program is shown as the program that performs the mathematical functions of each species of the argon chemical kinetic model. The main program created is named solvey.m, for input data programs with the names thtdata.m and odefunz.m. The data program thtdata.m contains the values for each species which are arranged based on the order of the reaction data in Table 1 to determine the values of the forward and reverse reactions. The input data is in odefunz.m contains boundary conditions in the form of pressure values, argon species loads, and temperature values that are the same for all species. In this research, the boundary condition is 1 times the atmospheric pressure, so the value used is 1 Atm. The main program solvey.m is the main program in the function model which is used as the output value of the mathematical solution in the thtdat.m and odefunz.m programs. In this program, several physical constants are used to convert units, then the solvey.m program will evaluate input data from thtdata.m and also odefunz.m.

3.5. Data Analysis

argon plasma modeling using MATLAB will present the density of argon plasma species at equilibrium conditions with a high-pressure value of 1 Atm. The species that will be involved in argon plasma are electrons, Ar, Ar^*, Ar^+, and Ar_2^+. In this modeling, several graphs of the density values of the argon plasma species at thermal equilibrium will be displayed, and also in the graphs, you will find out how long it takes for the argon plasma to reach equilibrium conditions.

4. RESULTS AND DISCUSSIONS

Argon plasma with the same electron temperature value and ion temperature value ($T_e = T_g$), with an integration time of $10^{-12} - 10^{-3}$ seconds, this time value is a reference for plasma equilibrium.

4.1. Argon Plasma Density Equilibrium

Thermal argon plasma modeling at atmospheric pressure involves five species that will be reviewed including e, Ar^*, Ar^+, Ar, and Ar_2^+. The input values, namely the input values of density, temperature, pressure, and integration time in this modeling are presented in Table 2.

Table 2. List of thermal argon plasma modeling input values.

Species	Density (m^{-3})	Temperature (eV)	Pressure (N/m^2)	Integration time (s)
Ar^*	1×10^4	2	1.01×10^5	$10^{-12} - 10^{-3}$
Ar^+	1×10^5	2	1.01×10^5	$10^{-12} - 10^{-3}$
Ar_2^+	1×10^6	2	1.01×10^5	$10^{-12} - 10^{-3}$
Ar	1×10^7	2	1.01×10^5	$10^{-12} - 10^{-3}$
e	1×10^{11}	2	1.01×10^5	$10^{-12} - 10^{-3}$

The equilibrium values of plasma argon species density are presented in Table 3.

Table 3. Argon species density at thermodynamic equilibrium.

Species	Initial density (m^{-3})	Final density (m^{-3})
Ar^*	1.3125×10^{16}	16.1181
Ar^+	3.2576×10^{11}	11.5129
Ar_2^+	1.6229×10^9	9.2103
Ar	6.5388×10^{13}	13.8155
e	4.057×10^{11}	11.6082

Equilibrium in argon plasma is achieved with the input values of density, pressure, and temperature in the plasma modeling which are shown in Figure 4. Figure 4 shows the modeling of thermal argon plasma experiencing density equilibrium with a time range of $10^{-12} - 10^{-3}$ seconds.
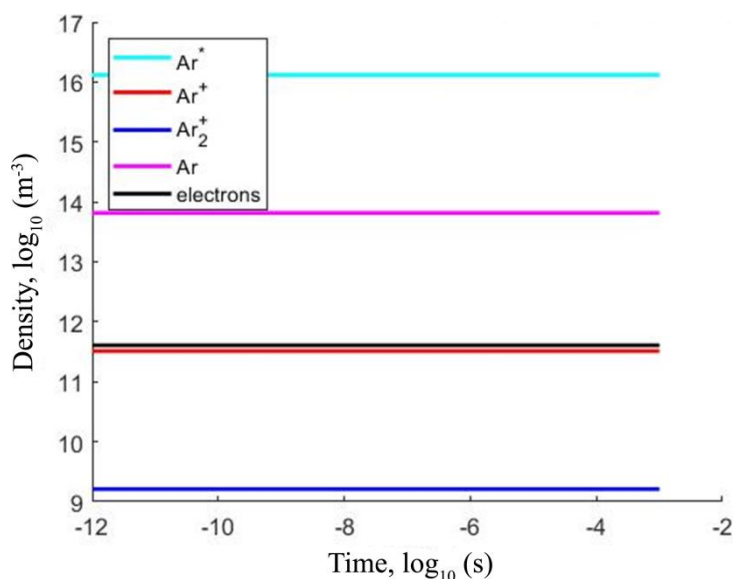

Figure 4. The density of argon species at 1 atm pressure.

4.2. Plasma Reaction Rate

This modeling calculates the reaction rate values for each reaction, the forward reaction rate, and the reverse reaction rate which are presented in Table 4.

Table 4. List of argon plasma modeling reaction rate values.

Reaction	Forward reaction rate ($m^{-3}.s^{-1}$)	Reverse reaction rate ($m^{-3}.s^{-1}$)
$e + Ar \rightarrow e + Ar^*$	2.046×10^{-5}	2.046×10^{-4}
$e + Ar^* \rightarrow e + Ar$	6.788×10^{-5}	6.788×10^{-4}
$e + Ar \rightarrow 2e + Ar^+$	6.793×10^{-6}	6.793
$e + Ar^* \rightarrow 2e + Ar^+$	2.482×10^{-1}	2.482×10^{4}
$e + Ar_2^+ \rightarrow Ar + Ar^*$	1.852×10^{-3}	1.683×10^{-4}
$e + Ar_2^+ \rightarrow e + Ar + Ar^*$	3.341×10^{-3}	3.037×10^{3}
$Ar^* + Ar^* \rightarrow e + Ar^+ + Ar$	6.20×10^{-4}	6.20
$Ar^* + Ar \rightarrow Ar + Ar$	3.00×10^{-10}	3.00×10^{-11}
$e + e + Ar^+ \rightarrow e + Ar$	3.867×10^{-22}	3.867×10^{-28}
$Ar^+ + 2Ar \rightarrow Ar + Ar_2^+$	4.194×10^{-30}	4.613×10^{-34}
$Ar + Ar_2^+ \rightarrow Ar^+ + 2Ar$	1.347×10^{-10}	1.347×10^{-11}

The reaction rate in this study is seen from the number of particles that will increase in volume and the magnitude of the species value. The largest reaction rate is shown by 4th order reaction, the reverse reaction rate is 2.482×10^{4} $m^{-3}.s^{-1}$, the smallest reaction rate is shown by 10th order reaction, the reverse reaction rate is 4.613×10^{-34} $m^{-3}.s^{-1}$. Argon plasma depends on the density of each argon species and the electron temperature is the same as the temperature of the other species [23-25].

4.3. Density Analysis of Argon Plasma Species at a Temperature of 2 eV

In this modeling, the initial density of each species is determined, namely Ar^*, Ar^+, Ar_2^+, Ar, and e, with the density value determined with a limit of 10^{27} $m^{-3}.s^{-1}$. Figure 5 shows that the density of Ar^* decreased exponentially after a period of running constant with the initial density input value being 10^7 m^{-3}, and when the equilibrium conditions were recorded in MATLAB, the density value of the excited argon species was 1.3125×10^{16} m^{-3}.

Equilibrium of argon plasma particles at high pressure (**Zakky et al.**)
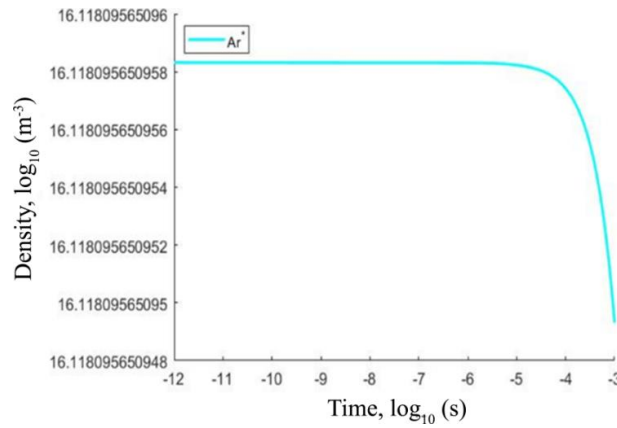
Figure 5. Density changes of excited argon.

Figure 6 shows that the basic state argon density was initially in equilibrium but after reaching equilibrium within a few moments it experienced a drastic increase. The initial input value was 10^6 m^{-3}, the value of the basic state argon density that occurred during the equilibrium conditions recorded in MATLAB The density log value obtained is 6.5388×10^{13} m^{-3}.
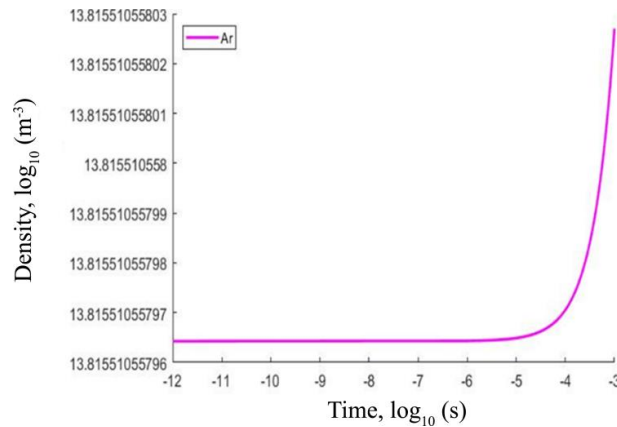

Figure 6. Changes in ground state argon density.

Figure 7 shows that the ion density of the Ar$^+$ was initially at equilibrium, but after reaching equilibrium within a few moments it experienced a drastic increase. The initial input value is 10^5 m^{-3}, the value of the density of the argon atomic ion which occurs during equilibrium conditions recorded in MATLAB, and the density log value is 3.2576×10^{11} m^{-3}.
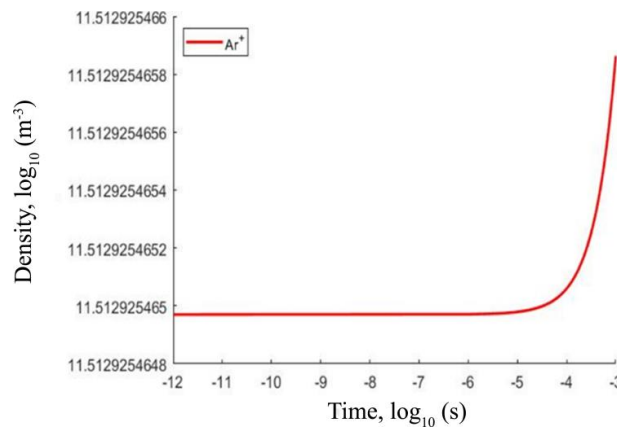

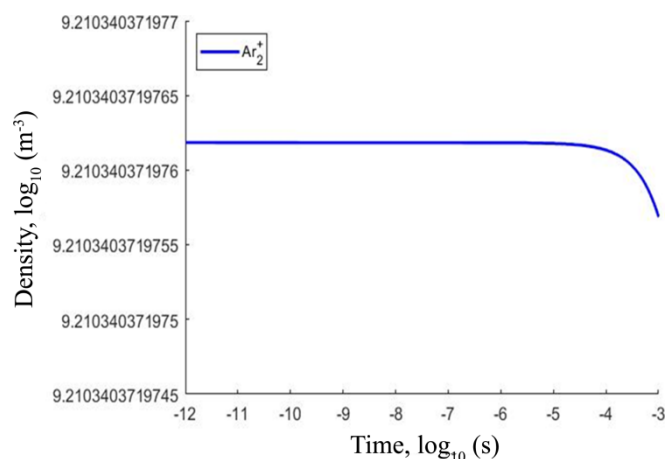Figure 7. Changes in the density of the argon atom.

Figure 8. Changes in density of argon molecular ions.

Figure 8 shows the results obtained that there was no significant change in the density of the Ar_2^+ species at the input value, namely 10^4 m^{-3}, for the density value of the argon molecular ion at equilibrium which was recorded as 1.6229×10^9 m^{-3}.
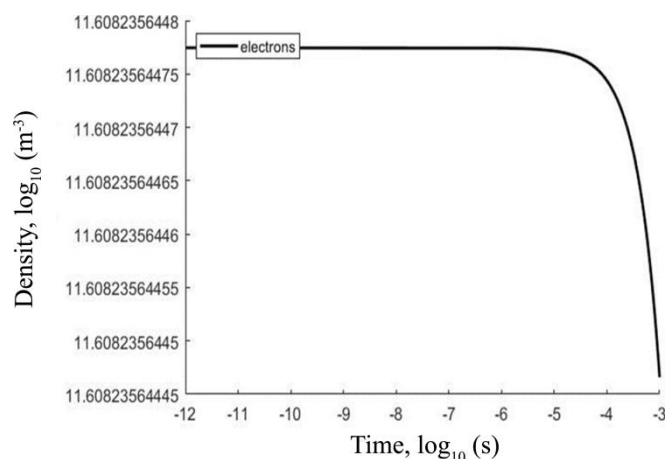

Figure 9. Change in electron density.

Figure 9 shows that for a few moments, there is a steady state of equilibrium, but a few moments later there is a quite drastic decrease in electron density. The initial input value of the electron density is the input value of the argon atomic ion plus the argon molecular ion ($Ar^+ + Ar_2^+ = 10^5 + 10^4$) which is 10^9 m^{-3}, for the log value of the electron density at the equilibrium moment obtained by the electron is 4.057×1011 m^{-3}.

5. CONCLUSION

Argon plasma has been modeled by many researchers, based on varying physical parameters. Several researchers such as Emmons and Weeks explained in their journal "Kinetic of High-Pressure Gas Discharge" in 2017 that argon gas is very good when the electron temperature is at 1 eV, the research carried out was at a temperature of 2 eV so the reaction process took a little longer.

In the process, the results of the modeling will decrease over time after experiencing equilibrium, this was also reported by Sode in his journal. Barker reported research that plasma equilibrium at atmospheric pressure with a gas composition of oxygen and nitrogen at a temperature range of 13000 Kelvin is in the time range of 10^{-3} seconds. By the results obtained, where the thermal argon equilibrium is in the time range $10^{-12} – 10^{-3}$ seconds.

REFERENCES
[1] Chen, F. F. (1984). *Introduction to plasma physics and controlled fusion*. NY: Plenum press.
[2] Yambe, K., Kuramoto, N., & Inagaki, Y. (2019). Dependence of plasma current on object condition in atmospheric pressure non-thermal equilibrium argon plasma. *AIP Advances*, **9**(8).
[3] Saktioto, S., Defrianto, D., Suhardi, S., Roslim, D. I., Awitdrus, A., Abdullah, H. Y., & Fadhali, M. M. (2023). Effect of chemical ions on oil palm midribs and leaves by direct electric voltage treatment. *Science, Technology and Communication Journal*, **3**(3), 71–78.
[4] Schneider, S., Lackmann, J. W., Narberhaus, F., Bandow, J. E., Denis, B., & Benedikt, J. (2011). Separation of VUV/UV photons and reactive particles in the effluent of a He/O2 atmospheric pressure plasma jet. *Journal of Physics D: Applied Physics*, **44**(29), 295201.
[5] Saktioto, S., Agustin, D., Zamri, Z., Basdyo, D., Abdullah, H. Y., Hairi, H. M., & Fadhali, M. M. (2023). Effect of direct current electric field on the root growth of oil palm seedlings. *Science, Technology and Communication Journal*, **3**(2), 51–56.
[6] Zissis, G., Charrada, K., & Stambouli, M. (1994). *Modelling the high pressure mercury discharge lamp warm-up* (No. CONF-940604-). IEEE Service Center, Piscataway, NJ (US).
[7] Devira, N. & Saktioto, T. (2022). Penggunaan pemodelan sumber plasma helium pada keadaan setimbang untuk aplikasi plak gigi. *Indonesian Physics Communication*, **19**(1), 11–18.
[8] Baeva, M., Bösel, A., Ehlbeck, J., & Loffhagen, D. (2012). Modeling of microwave-induced plasma in argon at atmospheric pressure. *Physical Review E—Statistical, Nonlinear, and Soft Matter Physics*, **85**(5), 056404.
[9] Alifah, S. N. & Saktioto, S. (2019). Kebergantungan temperatur plasma hidrogen dalam tekanan rendah. *Indonesian Physics Communication*, **16**(2), 118–122.
[10] Leonhardt, D., Walton, S. G., & Fernsler, R. F. (2007). Fundamentals and applications of a plasma-processing system based on electron-beam ionization. *Physics of plasmas*, **14**(5).
[11] Panicker, P. K. (2003). *Ionization of air by corona discharge*. University of Texas: Arlington.
[12] Eliezer, S. & Eliezer, Y. (2001). *The fourth state of matter: an introduction to plasma science*. CRC Press.
[13] Howling, A. A., Hollenstein, C., & Paris, P. J. (1991). Direct visual observation of powder dynamics in rf plasma-assisted deposition. *Applied Physics Letters*, **59**(12), 1409–1411.
[14] Tonks, L. (1967). The birth of "plasma". *American Journal of Physics*, **35**(9), 857–858.
[15] Fitzpatrick, T. (2014). *International handbook on social policy and the environment*. Edward Elgar Publishing.
[16] Rostoker, N. & Rosenbluth, M. N. (1960). Test particles in a completely ionized plasma. *Physics of Fluids*, **3**(1), 1.
[17] Kim, D. H., Park, C. S., Shin, B. J., Seo, J. H., & Tae, H. S. (2019). Uniform area treatment for surface modification by simple atmospheric pressure plasma treatment technique. *IEEE Access*, **7**, 103727–103737.
[18] Ansori. (2015). *Thermal and plasma deposition of electronic materials*. Paper Knowledge, Toward a Media History of Documents.
[19] Yubero, C., Dimitrijević, M. S., García, M. C., & Calzada, M. D. (2007). Using the van der Waals broadening of the spectral atomic lines to measure the gas temperature of an argon microwave plasma at atmospheric pressure. *Spectrochim. Acta B: At. Spectrosc.*, **62**(2), 169.
[20] Van Gaens, W. & Bogaerts, A. (2013). Kinetic modelling for an atmospheric pressure argon plasma jet in humid air. *Journal of Physics D: Applied Physics*, **46**(27), 275201.
[21] Nur, M., Bonifaci, N., Denat, A., & Atrazhev, V. M. (2015). Broadening of the spectral atomic lines analysis in high density argon corona plasma by using voigt profile. *Journal of Physics: Conference Series*, **622**(1), 012055.
[22] Park, J., Henins, I., Herrmann, H. W., Selwyn, G. S., Jeong, J. Y., Hicks, R. F., Shim, D., & Chang, C. S. (2000). An atmospheric pressure plasma source. *Appl. Phys. Lett.*, **76**(3), 288–290.
[23] Makabe, T. (2019). Metastables as a probe for low-temperature plasma characteristics in argon. *Journal of Physics D: Applied Physics*, **52**(21), 213002.
[24] Von Keudell, A. & Schulz-Von Der Gathen, V. (2017). Foundations of low-temperature plasma physics—An introduction. *Plasma Sources Science and Technology*, **26**(11), 113001.
[25] Murphy, A. B. & Uhrlandt, D. (2018). Foundations of high-pressure thermal plasmas. *Plasma Sources Science and Technology*, **27**(6), 063001.